

## Forum Review

# The Machinery for Oxidative Protein Folding in Thermophiles

EMILIA PEDONE,<sup>1</sup> DANILA LIMAURO,<sup>2</sup> and SIMONETTA BARTOLUCCI<sup>2</sup>

### ABSTRACT

Disulfide bonds are required for the stability and function of many proteins. A large number of thiol-disulfide oxidoreductases, belonging to the thioredoxin superfamily, catalyze protein disulfide bond formation in all living cells, from bacteria to humans. The protein disulfide isomerase (PDI) is the eukaryotic factor that catalyzes oxidative protein folding in the endoplasmic reticulum; by contrast, in prokaryotes, a family of disulfide bond (Dsb) proteins have an equivalent outcome in the bacterial periplasm. Recently the results from genome analysis suggested an important role for disulfide bonds in the structural stabilization of intracellular proteins from thermophiles. A specific protein disulfide oxidoreductase (PDO) has a key role in intracellular disulfide shuffling in thermophiles. Here we focus on the structural and functional characterization of PDO correlated with the multifunctional eukaryotic PDI. In addition, we highlight the chimeric nature of the machinery for oxidative protein folding in thermophiles in comparison with the mesophilic bacterial and eukaryal counterparts. *Antioxid. Redox Signal.* 10, 157–169.

### THIOL DISULFIDE OXIDOREDUCTASE

Disulfide bonds between cysteine pairs are among the major structural features of many proteins. Proteins capable of catalyzing protein disulfide bond formation include a large number of thiol-disulfide oxidoreductases, which occur in all living cells, from bacteria to humans. Thiol disulfide oxidoreductases are characterized by an active site containing a CXXC motif and by a thioredoxin (Trx) fold (five strands of  $\beta$  sheets enclosed by four  $\alpha$ -helices) (59). Trx, glutaredoxin (Grx), glutathione *S*-transferase (GST), disulfide bond-forming protein (Dsb)A (58), and protein disulfide isomerase (PDI) (20, 49, 50) constitute the large Trx superfamily. These proteins in different way contribute to the cellular redox environment, which is essential for the folding and stability of other proteins. Although Trx-like redox proteins or redox active domains share no overall sequence homology, they all contain a CXXC catalytic motif, which is located at the N terminus of the first helix in the consensus Trx fold (59), and a cis-Pro loop, which precedes the  $\beta 3\beta 4\alpha 3$  motif. At physiologic pH, the N-terminal cysteine of CXXC motif of the active site shows higher reactivity. This

residue is largely solvent exposed and has a low  $pK_a$ , acting as nucleophilic cysteine ( $R-S^-$ ), whereas the other is buried and has a higher  $pK_a$  value. The nature of the amino acids between these two cysteines varies widely among the different enzymes. Although these enzymes do have common features, they differ greatly in the  $pK_a$  values of the nucleophilic cysteine and in their redox potentials, ranging from  $-270$  mV for Trx to a value between  $-90$  and  $-125$  mV for DsbA.

### THE BACTERIAL MACHINERY FOR OXIDATIVE PROTEIN FOLDING

In gram-negative bacteria, disulfide bond formation is assisted by proteins of the Dsb family, which are either located in extracytoplasmic compartments or secreted into the medium. The Dsb family of oxidoreductases regulates the formation of disulfide bonds in the bacterial periplasm through two distinct electron-transfer pathways, the oxidation and the isomerization pathways (22, 45, 62). In the *Escherichia coli* oxidation pathway, DsbA

<sup>1</sup>Istituto di Biostrutture e Bioimmagini, C.N.R., and <sup>2</sup>Dip. Biologia Strutturale e Funzionale, University of Naples "Federico II", Complesso Universitario Monte S. Angelo, Naples, Italy.

introduces disulfide bonds into newly translocated proteins by donating its active-site disulfide bond. The active form of DsbA is restored by the inner-membrane protein DsbB, which uses the oxidizing power of the electron-transport system (32). Under aerobic conditions, electrons are passed from DsbB *via* ubiquinone and the cytochrome *bo* and *bd* oxidase to molecular oxygen. Under anaerobic conditions, DsbB uses menaquinone as an intermediate electron acceptor, from which electrons are transferred to either fumarate reductase or nitrate reductase (22, 45, 62). The disulfide oxidation step catalyzed by DsbA is rapid and nonspecific and, in proteins with multiple thiols, can result in the formation of nonnative disulfide bonds. The DsbC–DsbD pathway catalyzes the rearrangement of incorrect disulfide bonds, enabling proteins to fold correctly (88). In this pathway, the isomerase DsbC must be kept reduced in the oxidative environment of the periplasm, a requirement that is mediated by the membrane protein DsbD. Recent genetic studies suggested that Dsb homologue systems are also found in gram-positive bacteria (45, 82). In *Bacillus subtilis*, two putative extracytoplasmic proteins (DdbA and DdbD), which are homologues of Trxs, and two putative membrane proteins (DdbB and DdbC), which show sequence homology to *E. coli* DsbB, have been identified. Genetic evidence indicates at least three genes encoding proteins that play a role in disulfide-bond formation. Moreover, the identification of DsbA and DsbB homologues by BLAST searches in the protein databases of both gram-positive bacteria and the previously mentioned *B. subtilis* supports the assumption that gram-positive bacteria may comprise oxidative pathways similar to those of gram-negative bacteria.

## THE EUKARYOTIC MACHINERY FOR OXIDATIVE PROTEIN FOLDING

In eukaryotes, protein folding, modification, and quality control occur mainly in the endoplasmic reticulum (ER) (99). Whereas different compartments in plants, such as the cytosol, mitochondria, and chloroplasts, have their own protein-folding machinery, the ER is unique in that it produces proteins for other compartments of the cell. Newly synthesized polypeptide chains destined for the secretory pathway are translocated into the ER with the aid of signal-recognition particles (SRPs) and receptors. Various folding factors resident in the ER recognize nascent proteins; these folding factors include chaperones from the heat-shock protein family, peptidylprolyl *cis-trans* isomerases, many lectins and glycoprotein-modifying enzymes (2), and protein-folding catalysts from the PDI family, Ero family, and Erv family. On the basis of findings in yeast (27), it is estimated that approximately one third of all eukaryotic proteins pass through the ER on their way to maturity, including all cell-surface and secretory proteins and proteins located in compartments along the exocytic or endocytic pathways (2). The ER is also one of the few compartments in the eukaryotic cell where proteins can acquire disulfide bonds (the mitochondria are another). In eukaryotic cells, disulfide bond formation and rearrangement are catalyzed both by PDI, a protein localized in the ER, and by its homologues (23). The three-dimensional structure of yeast PDI has recently been solved (102). PDI is organized into four domains (a, b, b', and a') followed

by a C-terminal extension referred to as c. The a and a' domains contain one catalytically active CGHC motif each, whereas b and b' are redox inactive domains. The overall structure of yeast PDI has the shape of a twisted "U" with the a and a' domains at the ends of the "U" and the b and b' domains forming the base. Each domain adopts the thioredoxin fold with minor variations, and the two active sites face each other on the inside of the "U." PDI catalyzes the oxidation and shuffling of disulfides in substrate proteins. In turn, PDI is oxidized by the ER oxidoreductin proteins Ero1-La and Ero1-Lb in mammalian cells (13, 69), AERO1 and AERO2 in plants (21), and Ero1p (35, 36, 96), or the ER oxidase Erv2p (34, 95, 103) in yeast. ER oxidoreductins couple disulfide bond formation to reduction of molecular oxygen with the help of a bound flavin adenine dinucleotide cofactor. This cascade, which involves a series of protein–protein interactions, leads to the formation of native disulfides in substrate proteins (36, 96, 102).

## THIOREDOXIN/GLUTAREDOXIN, UBIQUITARIOUS REDUCTANTS

Trxs and Grxs, also included in the Trx superfamily of disulfide oxidoreductase, are small (~12 kDa) ubiquitous acidic proteins whose main function is to preserve redox homeostasis in the cytoplasm by acting as disulfide reductase in several biologic reactions, playing important roles in cellular responses, including cell growth, cell cycle, gene expression, and apoptosis (30, 40, 79). Both proteins contain the conserved motif (CXXC) in an active site to form a disulfide bond after reduction of exposed disulfides in a variety of substrate proteins. The reduced form is regenerated by the flavoenzyme thioredoxin/glutathione reductases, respectively, which in turn are kept reduced by NADPH (39). Furthermore, these proteins function as electron donors for the ubiquitous family of Trx peroxidases or peroxiredoxins (Prx) involved in the defense against oxidative damage (91).

The active-site sequence —WCGPC— is highly conserved in Trxs, whereas Grxs have the conserved —CPYC— in all but two members (T4-Grx has a Val in place of Pro, and Pig-Grx has a Phe in place of Tyr).

As a general rule, significant differences exist between Trxs and Grxs at their N-termini, where the former typically has additional 15 to 20 residues. These extra residues form well-defined secondary structures that lie on either side of the central  $\beta$ -sheet core, not implicated in the redox functionality of these proteins. In addition the Grx fold is slightly different from the Trx fold, being constituted by central four-stranded  $\beta$ -sheet core surrounded by two helices on one side and a third on the other.

## THE CHIMERIC PATHWAY FOR OXIDATIVE PROTEIN FOLDING IN THERMOPHILES

### *The ancestral Trx and Grx from methanogenes*

MtH0895 is a small 77-residue protein identified in 1992 from the thermophilic archaeon *Methanobacterium thermoau-*

*totrophicum* as a conserved hypothetical protein with unassigned function (60). Because of its small size and good solution behavior, this protein was chosen for detailed structural analysis by NMR spectroscopy (9). In addition, as the solution structure was determined, it became obvious that *MtH0895* exhibited a Grx-like fold. *MtH0895* does not contain the additional N-terminal secondary structural elements, suggesting that it is more like a Grx. The suspicions were raised about the true function of this protein when a literature search revealed that *M. thermoautotrophicum* does not contain glutathione or a glutathione-like cytosolic thiol (9), essential for Grx function. To confirm the suspicions, a detailed investigation was undertaken to determine the true nature of *MtH0895* through sequence, structural, and biochemical analysis. Little similarity is found in the primary sequences between *MtH0895* and the members of the Trx superfamily. Sequence comparisons between *MtH0895* and "standard" Trxs indicate that only a few residues are fully conserved. These include the two active-site cysteines, a *cis*-proline at the loop preceding  $\beta 3$ , a glycine residue between  $\beta 3$  and  $\beta 4$ , and a second glycine immediately after  $\beta 4$ . *MtH0895*, however, has a unique -CANC- motif, which is not found in any known member of the Trx or Grx superfamily. It is believable that the absence of a Pro residue in the *MtH0895* active site may confer some conformational flexibility and therefore may have some effect on the stability of the redox-reaction process in this enzyme. Detailed analysis of its three-dimensional structure along with molecular docking simulations of the interaction with T7 DNA polymerase (a Trx-specific substrate) and comparisons with other known members of the Trx/Grx family of proteins strongly suggest that *MtH0895* is more akin to a Trx. Furthermore, measurement of the  $pK_a$  values of its active-site thiols along with direct measurements of the Trx/Grx activity has confirmed that *MtH0895* is, indeed, a Trx and exhibits no Grx activity.

A group of previously unknown proteins from several other archaea that have significant (34–44%) sequence identity with *MtH0895* were also identified. These proteins have unusual active site -CXXC- motifs not found in any known Trx or Grx. On the basis of the results, it was predicted that these small proteins are all members of a new class of truncated Trx functioning essentially as Trxs rather than Grxs and exhibiting no activity as glutathione mixed disulfide reductants (53, 60).

*MtH0807* is another 85-residue thiol-redox protein isolated from the same anaerobic archaeon *M. thermoautotrophicum*. Its small size, its participation in certain redox reactions, and the presence of a "classic" Grx active-site sequence led to the suggestion that it might be a Grx. However, preliminary studies indicated that it exhibited neither Grx-like nor Trx-like properties. To clarify the true role of this protein and its structure/functional relation with the paralogous Trx (*MtH0895*, 28% sequence identity), a series of biochemical and biophysical studies was undertaken. Comparative enzymatic assays and thiol titration experiments were combined with NMR structural studies and detailed 3D structure comparisons (1). Structurally, the results show that *MtH0807* has a Grx-like fold (central four-stranded  $\beta$ -sheet core surrounded by two helices on one side and a third on the other). However, more-detailed comparisons with other members of the Trx superfamily indicate that *MtH0807* has several key structural and active-site characteristics more similar to a Trx. Furthermore, biochemical tests show

that *MtH0807* behaves as a true Trx. The absence of Grx activity could be due to absence of glutathione (GSH) in *M. thermoautotrophicum* (9, 53, 60). When glutathione became more abundant 1 to 2 billion years ago (26, 61), *MtH0807*-like proteins could have evolved toward a Grx function, by using GSH to provide the reducing equivalents for ribonucleotide reductase for DNA synthesis. The relatively small number of residue changes (*i.e.*, two positively charged residues around the active site) that may be needed to convert *MtH0807* to a fully functional Grx (60) suggests that the evolutionary process may have been relatively quick and easy.

Comparisons between *MtH0807* and its paralogue, *MtH0895*, indicate that these two archaeal Trxs share very similar folds, but exhibit very different activities and likely serve somewhat different roles. On the basis of its greater relative abundance and significantly stronger redox activity, it may be that *MtH0807* is the primary Trx for *M. thermoautotrophicum*, whereas *MtH0895* plays a minor or supportive role. These two molecules (*MtH0807* and *MtH0895*) may represent a group of ancient proteins that were ancestral to both Trxs and Grxs. An important question that may be asked is why does a simple archaeon like *M. thermoautotrophicum* have two Trxs? It is important to note that most eubacteria and all eukaryotes have both Trxs and Grxs encoded in their genomes. This redundancy in redox function for these organisms may have arisen because the activities sustained by Grx and Trx (DNA synthesis, transcriptional control, and protein-function regulation) are so essential to an organism's viability (39). The same may be true for *M. thermoautotrophicum* and other archaea. Structural characterization and biochemical-assay comparisons between *MtH0807* and *MtH0895* indicate that both proteins have similar structures, and both use the same reducing system (the Trx system). *MtH0807* is, however, more oxidative and seem to have very little reductive ability as compared with *MtH0895*. Evidence suggests that *MtH0807* is the much more abundant protein in *M. thermoautotrophicum*, especially when grown under native-like anaerobic conditions (60). The strong reducing environment in which this organism thrives (53) suggests the need for a strongly oxidizing form of Trx to provide the reducing equivalents to ribonucleotide reductase for DNA synthesis. It appears that *MtH0807* fills the bill. In contrast, *MtH0895*, which is the less abundant protein, may be a "backup" to *MtH0807*, or it may be involved in other, less important disulfide redox activities within the cytoplasm. Alternately, *MtH0895* may be the Trx produced when *M. thermoautotrophicum* is exposed to more aerobic conditions. Although both *MtH0895* and *MtH0807* are true Trxs, in some respects, *MtH0807* seems to play the role of a Grx (with its strong oxidizing potential and other physical features), whereas *MtH0895* seems to play the role of a Trx. Given the "archaic" nature of archaea and their hypothesized role in eubacterial and eukaryotic evolution, *MtH0807* and *MtH0895* may be molecular "fossils" representing an early branch point in the evolution of Grxs and Trxs. In *Methanococcus jannaschii*, another Trx-like protein (Mj0307) with a —CPHC— in the active site, which had never been observed in either Trxs and Grxs, and a thioredoxin reductase homologue were identified. The Trx-like protein exhibits biochemical activities similar to those of Trx, although its structure is more similar to Grx. This protein presents the lowest value so far known among redox potentials of the Trx

superfamily (60). This indicates that the lower redox potential is necessary to keep catalytic disulfide bonds reduced in the cytoplasm; moreover, the experimental data suggested that a Trx-like protein with a Grx-like structure is enough to maintain redox homeostasis in methanogens like *M. jannaschii* and *M. thermoautotrophicum*.

### Trx/Grx from thermophilic microorganisms

The Trx of *Alicyclobacillus acidocaldarius* (*BacTrx*) is the first Trx so far described from a thermophilic source (5). Structural stability investigated by CD, DSC, and nanogravimetry have demonstrated that it is endowed with a higher conformational heat capacity when compared with the Trx from *E. coli* (*EcTrx*), showing a denaturation temperature (105°C) 15°C higher than *EcTrx*, which is itself a remarkably stable molecule (70, 71). The comparison with other Trxs, such as Trx-2 from a cyanobacterium of the *Anabaena* genus (94), Trx h from the eukaryotic green alga *Chlamydomonas reinhardtii* (54), and human Trx (11), showed that *BacTrx* model is closer to bacterial and cyanobacterial Trxs than to eukaryotic ones. As also pointed out by Mittard *et al.* (64), the superimposition of thioredoxins from different sources clearly reflects their phylogenetic relation. The *BacTrx* 3D structure (Fig. 1), determined by NMR methods, was compared with *EcTrx*, determined by x-ray crystallographic diffraction, and a number of structural differences observed could contribute to its thermostability. The results of

structural analysis indicated that protein stability is due to cumulative effects: an increased number of ionic interactions cross-linking different secondary structural elements and clamping the C-terminal  $\alpha$ -helix to the core of the protein, leading to a more rigid structure. In comparing the primary structure of Trx from thermophilic sources (68, 70–72) with *EcTrx*, no great differences seem to be found (Fig. 2), justifying any way differences in stability as 15°C with *BacTrx*. More in detail flexible residues, such as Gly21, Gly65, and Gly97, found in *EcTrx*, are never found in the same position in any thermophilic Trxs. In addition, no charged residues, as well as D102 in *BacTrx*, are found in the C-terminal tail of *EcTrx*. This feature is fundamental because it is assumed that the C-terminal helix plays a protective role on the whole molecule because of the multiple ionic interactions with residues located in the protein core.

To investigate further the determinants of protein stability, four mutants of *BacTrx* were designed, *i.e.*, K18G, R82E, K18G/R82E and D102X, in which the last four amino acids were deleted (71). These were constructed on the basis of molecular dynamics studies and the prediction of the structure of *BacTrx* performed by a comparative molecular-modeling technique by using *EcTrx* as the reference protein.

The mutants obtained by PCR strategy were expressed in *E. coli* and then characterized. CD spectroscopy, spectrofluorimetry, and thermodynamic comparative studies allowed us to determine the relative physicochemical behavior of the four proteins in comparison with that of the wild-type protein (Table 1). As predicted for the molecular dynamics analysis at 500 K *in vacuo*, the wild-type structure is more stable than that of the mutants; the *T<sub>m</sub>* of the four proteins shows a decrease of ~15°C for the double and the truncated mutants, and ~12°C for the single mutants. The proteins also revealed a different resistance to denaturants such as guanidine HCl and urea, and the wild-type protein always proved the most resistant. The results obtained show the importance of hydrogen bonds and ion pairs in determining protein stability and confirm that simulation methods are able to direct protein engineering in site-directed mutagenesis (7, 73).

A Trx from the thermophilic bacterium *Thermus thermophilus* was isolated, and its structure solved to 1.8-Å resolution (83). The folded portion of this Trx is in a more compact form than standard Trxs, although this protein contains, like other Trxs from thermophilic microorganisms, a 30-residue N-terminal extension and a significantly longer C-terminal  $\alpha$ -helix.

In the genome database of the aerobic hyperthermophilic archaeon *Aeropyrum pernix* K1, a new gene that codes for a 37-kDa protein (*ApTrx*) with a redox-active site motif (CPHC) was found (43). *ApTrx* is larger in size than the other Trx homologues because of an extended region at the N-terminus. This region showed no homology to sequences in the databases, and the function is unknown. The active-site motif is the same as that of *E. coli* DsbA, the most powerful oxidant among thiol-disulfide oxidoreductases (108). The two central residues within the active site motif play a critical role in determining the redox potential (31). Nevertheless, the redox potential of *ApTrx* is -262 mV, which is very different from that of *E. coli* DsbA (-125 mV). This indicates that amino acids other than those within the active site are also

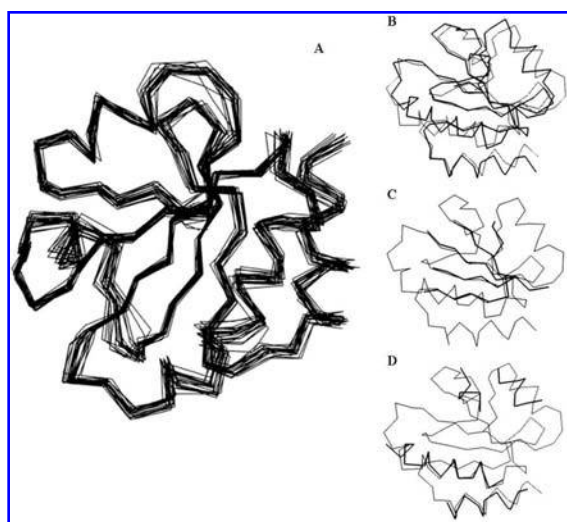


**FIG. 1. (A) Family of the 20 solution structures representative for *BacTrx*.** The structures, superimposed for minimal RMSD of the backbone atoms N,  $\alpha$ , and C' of residues 2–105, are represented as  $\alpha$  traces. **(B)** Comparison of the tertiary structures of *BacTrx* (thin lines) and *EcTrx* (bold lines). **(C)** Superimposition of the  $\beta$ -strands of *EcTrx* (bold lines) onto a representative *BacTrx* structure (thin lines). **(D)** Superimposition of the  $\alpha$ -helices of *EcTrx* (bold lines) onto a representative *BacTrx* structure (thin lines). The molecules represented as  $\alpha$  trace were superimposed with the main-chain atoms (N,  $\alpha$  and C') (residues 5–104 with 7–106 for *BacTrx* and *EcTrx*, respectively). The sequences were aligned by a least-squares fit of  $\alpha$ -trace.



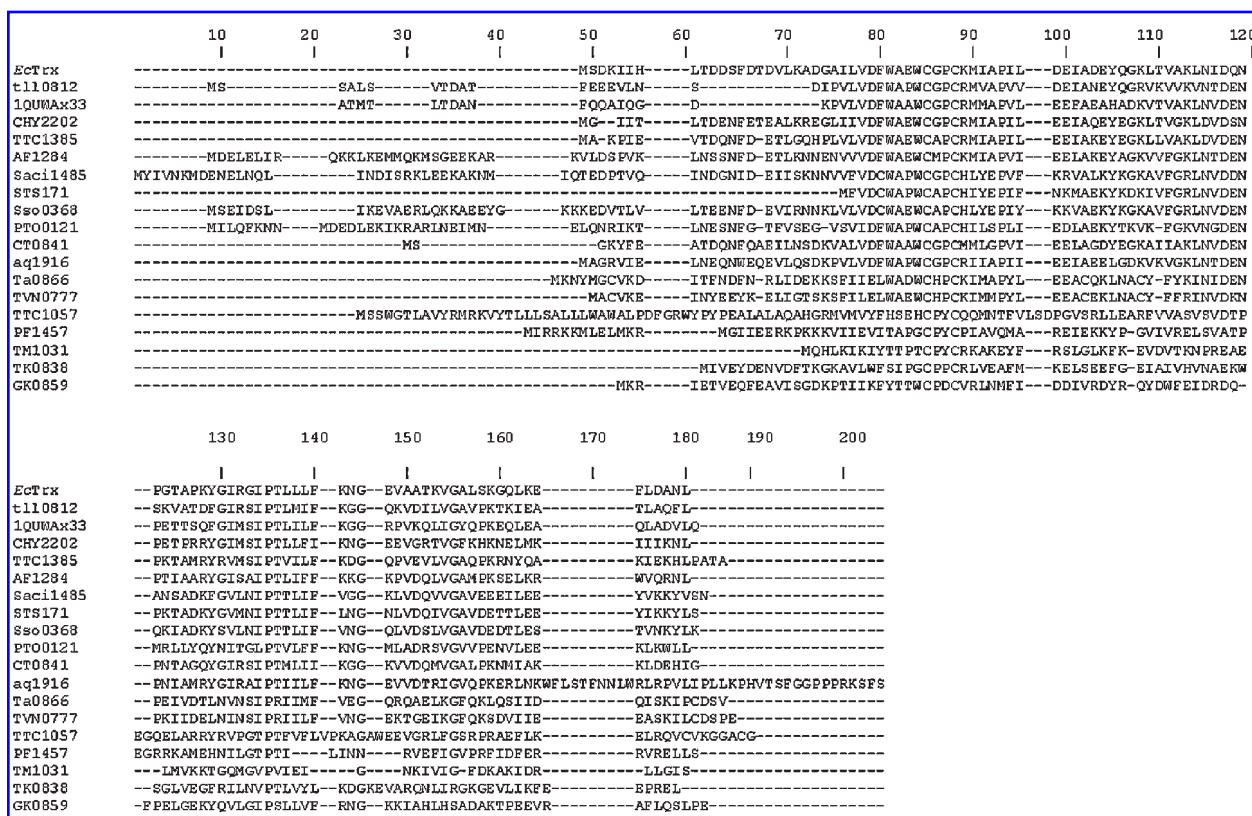


**FIG. 2. Primary structures of thermophilic Trxs and their homologues.** Trxs of the same size have been chosen excluding methanogenes and taking only one Trx from each source. Trx sequence data were taken from the following genomic sources: EcTrx from *Escherichia coli*, tll0812 from *Thermosynechococcus elongates BP-1*, 1QUAx33 from *A. acidocaldarius*, CHY\_2202 from *Carboxydotherrmus hydrogenoformans*, TTC1385 from *Thermus thermophilus HB2*, AF1284 from *Archaeoglobus fulgidus DSM 4304*, Saci1485 from *S. acidocaldarius DSM 639*, STS171 from *S. tokodaii str. 7*, Sso0368 from *S. solfataricus P2*, PTO0121 from *Picrophilus torridus DSM 9790*, C0841 from *Chlorobium tepidum*, aq\_1916 from *A. aeolicus*, Ta0866 from *Thermoplasma acidophilum DSM 1728*, TVN0777 from *Thermoplasma volcanium GSSI1*, TTC1057 from *T. thermophilus HB27*, PF1457 from *P. furiosus*, TM\_1031 from *Thermotoga maritima*, TK0838 from *Thermococcus kodakarensis KOD1*, and GK0859 from *Geobacillus kaustophilus HTA426*. In red are showed cysteines of active sites.

important in determining redox potential (90) and that the lower redox potential is necessary to keep catalytic disulfide bonds reduced and to cope with oxidative stress (53). However, ApTrx exhibits biochemical activities similar to classic Trxs. ApTrx contains two extra cysteine residues, but its activity is not affected by preincubation with dithiothreitol, indicating that the activity of ApTrx is not dependent on the redox state of the protein. *A. pernix* results to have multiple Trx-like proteins similar to ApTrx justified by a peculiar role

of the redox system in *A. pernix* in different growth or stress conditions (43).

Investigations of the genomic-sequence databases of *Sulfolobus solfataricus* led to the identification of two putative Trxs with a deduced molecular mass of 15.228 Da and 15.220 Da, respectively [i.e., SsTrxA1 and SsTrxA2 (Sso0368 and Sso2232)] (77). In the tested conditions, both of these Trxs proved to be inactive in the DTNB-coupled reduction with a thioredoxin reductase Sso2416 from *S. solfataricus* (SsTR). Se-

TABLE 1. DENATURATION VALUES OF WILD-TYPE AND MUTANTS BACTrx

	<i>T<sub>m</sub></i>	<i>T<sub>m</sub></i> + 1M GuCl	<i>T<sub>m</sub></i> + 2M urea	Urea (M)	GuCl (M)
BacTrx	103	84.5	88.2	6.7	2.9
K18G	91	78.1	78.8	5.2	2.6
R82E	91	81.5	81.4	5.5	2.7
K18G/R82E	89	76.3	73.1	4.6	2.4
D102X	86	65.2	70.6	4	2

The values were calculated on the presence of temperature or temperature plus 1 M guanidine HCl or temperature plus 2 M urea or guanidine HCl or Urea.

quence analysis showed that *SsTrxA1* and *SsTrxA2* present ~30% identity with the well-characterized Trxs of *E. coli*, Trx1 and Trx2, used as substrates for *E. coli* TR. Several structurally and functionally important amino acids conserved in various Trxs were seen to be conserved in both these *SsTrxs* as well. They include (Trx1 numbering) Trp28, Cys35 and Cys 38 (redox cysteines), Pro40 (maintains the conformation of the redox disulfide of Trx), Tyr49, Lys/Arg57 (influences the pK<sub>a</sub> of active Trx cysteines), Asn59 and Asp/Glu61 (clustered with the redox active site of Trx), Ala67 and Ile/Val75 (structural), Pro76 (in van der Waals contacts with the Trx disulfide bridge), Thr77 and Gly84 (structural), and Gly92 (protein-interaction area).

### *Disulfide-bonded proteins in thermophiles: PDO, a primary catalyst of disulfide bond formation in thermophiles*

Thermophilic microorganisms include inhabitants of fairly extreme environments. One way to adapt to harsh surroundings is to evolve proteins to be resistant to inactivation from various extreme conditions. It now appears that, at least for some thermophiles, this evolution has resulted in the unusual situation in which large numbers of cytoplasmic proteins are disulfide bonded (8, 57), indicating that disulfide bond formation plays a critical role in the structural stabilization of intracellular proteins. These findings raise the question of what kind of cytoplasmic system catalyzes the formation of disulfide bonds in these microorganisms. In thermophilic organisms, a potential key role in disulfide bond formation has recently been ascribed to a new cytosolic protein disulfide oxidoreductase (PDO) family (74, 76), whose members have a molecular mass of ~26 kDa and are characterized by two Trx folds comprising a CXXC active-site motif each. Notably, proteins from this family were not observed in certain key organisms, such as *M. jannaschi*, *Methanococcus kandleri*, and *Archaeoglobus fulgidus*. Therefore, its precise correlation with richness in protein intracellular disulfides can be considered strong evidence for a true relation to this cellular property. As this family plays a major role as a cytoplasmic system in catalyzing the formation of disulfide bonds, it provides a basis for further elucidating of protein-folding mechanisms in such microorganisms.

Investigation into genomic-sequence databases indicated that members of PDO family are present only in thermophilic microorganisms. Three members of this family have been characterized from both the structural and functional points of view. One was isolated from the archaeon *Pyrococcus furiosus* (*Pf*-PDO) (6, 24, 84–86), another from the bacterium *Aquifex aeolicus* (*Aa*PDO) (16, 76), and one from the archaeon *A. pernix K1* (*Ap*PDO) (18). All these enzymes were found to be organized into two structural units. Although these two structural units can be functionally related to the active domains of the eukaryotic enzyme PDI, unlike those of PDI, they pack tightly together and are thus structurally unseparated. Recently another member from *S. solfataricus* (*Ss*PDO) has been characterized *in vitro* and *in vivo* (77).

### *Pf*PDO

The first member of the PDO family studied from both the structural and functional points of view was *Pf*PDO. The analysis of the crystal structure showed that it was composed of two structural units containing one CXXC motif each (Fig. 3): a CQYC sequence, which has never been observed in any other protein disulfide oxidoreductase, is present at the N-terminal half of the protein, and a CPYC, the conserved active sequence of the Grx, located at the C-terminal half of *Pf*PDO, which could explain why this protein has been initially classified as Grx (37). An uncommon combination of two Trx-related structures, which together, in tandem-like manner, formed a closed protein domain with a central eight-stranded  $\beta$ -sheet constituting the protein core and eight  $\alpha$ -helices distributed asymmetrically on both sides of the central sheet was observed. The two active sites exhibited markedly different geometric parameters and solvent accessibilities. The N-terminal site was completely buried and showed unusual dihedral angles, which were indicative of unfavorable disulfide bond conformation. In contrast, the C-terminal site had a stable and exposed disulfide bond (85). The structural comparison with other PDO proteins showed that each of the structural units in *Pf*PDO is a Trx fold motif, albeit with the insertion of an additional  $\alpha$ -helix ( $\alpha 1$  or  $\alpha 5$ ) at the N-terminus. Their sequence identity is rather low: the N-unit is only 18% identical to the C-unit.

*Pf*PDO was demonstrated to be able to catalyze the oxidation of dithiols, as well as the reduction and the rearrangement of disulfides. In the presence of GSH, up to 70°C, *Pf*PDO catalyzes the formation of a disulfide bond between the two cysteines of the peptide NRCSQGSCWN, an activity similar to that observed for DsbA at 25°C (92). At 30°C, *Pf*PDO is able to catalyze the reduction of insulin disulfides in the presence of dithiothreitol. The disulfide rearrangement was also observed at a similar temperature by using RNase with scrambled disulfides as substrate.

The first cysteine of each redox site was mutated to investigate the effect on the protein function. By using the two single mutants (C35S and C146S) and the double mutant (C35S/C146S), the C-terminal site of *Pf*PDO was demonstrated to be determinant for the reductive activity. This result is in agree-

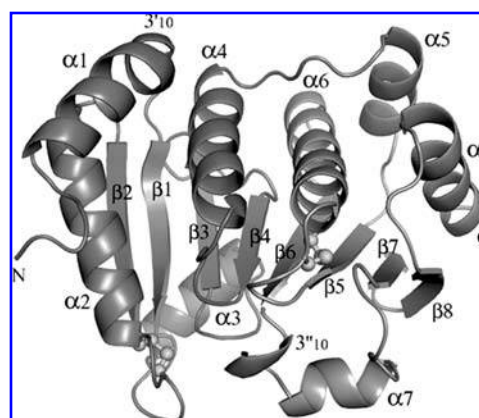


FIG. 3. Ribbon diagram of the PDO from *P. furiosus*.

ment with crystallographic data, which suggested a reductive nature for the C-unit (74, 85). The lower capacity of the N-unit to reduce disulfuric bridges can be due to intrinsic factors, such as a higher redox potential and a major conformational tension of the disulfide, but it could also depend on external factors such as steric impediments caused by a closed conformation of the active site in the N-unit. As regards the oxidative activity, the two units also display differences in their functional properties, with the site at the C-terminal always predominant, because at 50°C, the mutant with a nonmutagenized site at the N-terminal shows a very low activity. Higher temperatures, closer to the physiologic temperature at which the microorganism *P. furiosus* lives, may be necessary to get more kinetic energy and to allow an open conformation at the site. Otherwise, a different substrate may be required because of the polar nature of the amino acids close to the active site. Conversely, both sites are necessary to the disulfide isomerase activity. Only the wild-type *Pf*PDO is able to refold scrambled RNase. This is in agreement with a functional model of PDI in which the domains function synergically (25, 49). As reported earlier, the emerging model of PDI comprises four structural domains, a, b, b', and a', plus a linker region between b' and a' and a C-terminal acidic extension. In this model of PDI function, individual domains with specialized roles contribute to different activities to catalyze complex isomerizations in substantially folded protein substrates. Mutations at the first cysteine of the active site in either the amino- or carboxyl-terminal thioredoxin domain inhibit the capacity of PDI to catalyze thiol-disulfide exchange reactions *in vitro*, reducing enzymatic activity to negligible levels. The redox/isomerase activities of PDI, as in Trx, are due to the reactivity of the N-terminal Cys residue in two Trx-like boxes (-CGHC-) within the a and a' domains of the protein (19). *Pf*PDO resembles eukaryotic PDI, as it has two Trx-like motifs. In PDI, the Trx-like regions are separated from each other in the primary structure, whereas in *Pf*PDO, they are connected directly. The fact that similar functional results have been obtained for *Ph*PDO, another PDO of the same family isolated from the archaeon *P. horikoshii* (47), indicates that the Trx units of the archaeal members of this new protein family are neither equivalent nor identical with the a and a' domains of PDI in either functional or structural terms.

The effect of pD and temperature on the structure and stability of *Pf*PDO was investigated with molecular dynamic (MD) simulations and FT-IR spectroscopy (75). pD affects differently the thermostability of  $\alpha$ -helices and  $\beta$ -sheets. The experiments allowed us to detect a secondary structural reorganization at a definite temperature and pD, which may correlate with a high ATPase activity of the protein detected at 90°C and at basic values (not far from its physiologic pH value) (74). FT-IR experiments conducted at pD 10.0 showed a protein structural reorganization at this value of pD. The FT-IR and computational results may suggest that the protein undergoes partially unfolding with a concomitant relaxation of the tertiary structure, followed by a reorganization of part of the structure in a new  $\beta$  conformation. This reorganization could explain the ATPase activity for *Pf*PDO at that pH. The property of *Pf*PDO to bind and hydrolyze ATP supports its correlation to PDI (81). An ATP-binding site and an ATPase activity related to its chaperone role have been reported in PDI (38). The ATPase activity

does not seem to be linked to the isomerase or redox activities. This is in full agreement with a report stating that the site of phosphorylation, and thus probably the ATPase active site, lies somewhere within the central domain of the PDI, and that this site is far away from the redox active sites in the sequence. In addition, the computational analysis underlines that the  $\alpha$ -helix regions are more sensitive to increases of pH and temperature with respect to the  $\beta$ -sheets.

### *Aa*PDO

Subsequently, a detailed characterization of another member of this family, *Aa*PDO, was reported in the literature (16, 76). Like *Pf*PDO, this protein was able to reduce, oxidize, and isomerize disulfide bridges at a high degree of catalytic efficiency and is thus the first example of a bacterial disulfide isomerase not belonging to the Dsb family. Unlike the C- and N-terminal active sites of the archaeal members *Pf*PDO and *Ph*PDO, those of *Aa*PDO, CESC, and CGYC are able to perform all the catalytic functions, although with nonequivalent contributions. Three active-site mutants, C34S, C148S, and C34S/C148S, were cloned, expressed, and functionally characterized. The results indicated that unlike the double mutant, the two single mutants were able to perform all the catalytic functions of the enzyme and that the two active sites had similar functional properties. This catalytic similarity was also reflected at the structural level: the two active-site disulfides were similar in terms of accessibility and had comparable structural features compatible with stable disulfide bonds (76). These findings provide evidence that the two active sites of *Aa*PDO perform catalytic functions and operate independently, in that either center alone imparts activity to the enzyme. Taken together, these results suggest that the two structural units of *Aa*PDO can reliably represent the a and a' domain of the eukaryotic PDI. Although recent years have seen a tremendous increase in literature data on PDI, the list of what we do not know about this enzyme is still long. The results obtained indicate that *Aa*PDO is the most PDI-like prokaryotic protein known so far.

### *Ap*PDO

A catalytic characterization of the archaeal *Ap*PDO was provided, besides performing structural analyses and computational studies (18). The functional characterization demonstrated that *Ap*PDO is able to catalyze the reduction, oxidation, and isomerization of disulfide bonds, as are all the other members belonging to PDO family. The enzyme structural analysis showed that it is made up of two structural units with a Trx fold, which contain a CXXC motif each, CETC and CPYC at N-terminal and C-terminal units, respectively, as had been observed for previously characterized members of this family (76, 85). The two CXXC disulfides have similar dihedral angles typical of a stable conformation.

To shed light on the catalytic properties of each CXXC motif, the theoretic pK<sub>a</sub> values of the cysteines were determined (Table 2). In the literature, it had been widely reported that the pK<sub>a</sub> values of the two cysteines were related to the redox potential of the active site, thus playing a critical role in the determination of the physiologic functions of the members of the

TABLE 2. ESTIMATED  $pK_a$ S FOR THE ACTIVE SITE CYSTEINES COMPUTED ON ApPDO, AaPDO, AND PfPDO

		ApPDO	AaPDO	PfPDO
N-terminal site	Cys1	9.2	9.5	12.0
	Cys2	25.4	23.0	26.5
C-terminal site	Cys1	7.3	6.0	8.0
	Cys2	>30	26.9	25.3

Trx superfamily (31, 51, 52). The results showed that the  $pK_a$  values of the N-terminal cysteines (Cys1) of both the active sites were similar and lower than those observed for the C-terminal cysteines (Cys2), thus suggesting that both ApPDO active sites were able to perform catalytic functions (67). At this point, the theoretic values of the cysteine  $pK_a$ s in AaPDO and PfPDO were also determined. Similar results to those obtained for ApPDO were obtained for AaPDO; the low  $pK_a$  values observed for the N-terminal cysteines of the two active sites are in agreement with the experimental observation that both of them perform catalytic functions (17). Different results were obtained for PfPDO: the  $pK_a$  value of the first cysteine of the N-terminal CQYC motif was particularly high, thus suggesting the inability of this site to perform the catalytic function. These data are in agreement with mutagenesis and kinetic studies, indicating that this site is less predisposed to any reductive or oxidative activity. These results suggest that despite similar functional and structural characteristics, the members of the PDO family greatly differ in terms of the contribution of each active site to total catalytic activity (Fig. 4).

### SsPDO

PDOs from the hyperthermophilic archaeon *S. solfataricus* were analyzed in a general research project to provide insight into the functions, structural diversity, and evolution of PDOs. Among hyperthermophilic archaea, *S. solfataricus* is a good model system, both because it is easily grown in aerobic condition and because the database recently created by the sequencing of its genome (97) has promoted notable advancements in genetic and molecular understanding.

The analysis of the complete sequenced *S. solfataricus* P2 genome (97) has revealed that the protein encoded by the ORF Sso0192 (SsPDO) is a homologue of PfPDO because it has two redox sites, CQYC and CPYC, respectively, located at the N- and C-terminals and a deduced molecular mass of ~26 kDa (77). Secondary structure previsions confirm the homology with the other members of PDO family. SsPDO displays several protein oxidoreductase activities, significantly lower than those of its homologue PfPDO. The lower efficiency can probably be traced to the lower redox efficiency of its cysteines and, possibly, to a modulation of its activity by conformational changes induced by substrates, cytoplasmic cofactors, or physiologic conditions. Moreover, a GSH-dependent low thiol-transferase activity of SsPDO and the absence of genes encoding glutathione synthesis enzymes, such as glutamylcysteine synthetase or a glutathione synthetase homologue, strongly suggest that SsPDO is not involved in any glutathione-dependent sys-

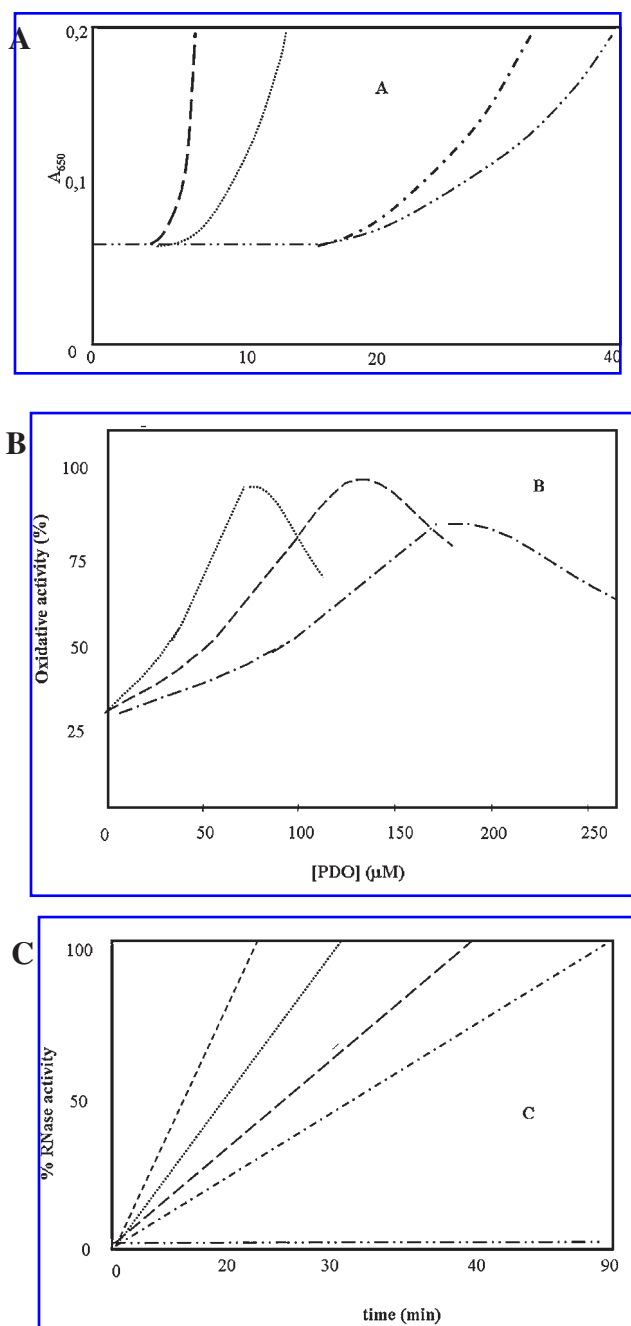


**FIG. 4. (A) Reduction of insulin catalyzed by PDOs:** PfPDO (—); AaPDO (·····); ApPDO (— · —); control (— — —). **(B)** The disulfide bond-forming activity of PDOs is monitored by using the synthetic decapeptide NRCSQGSCWN, and the oxidation of this dithiol peptide to the disulfide state is accompanied by a change in time retention on a Vydac C18. The oxidative activity is reported as a ratio between the peak of oxidized versus oxidized plus reduced peptide. The assays of oxidative activity were performed at 323 K, with an incubation time of 30 min, at increasing concentrations of PDOs. PfPDO (—); AaPDO (·····); ApPDO (— · —). **(C)** Assay of isomerase activity of PDOs by reactivation of “scrambled” ribonuclease A. The recover of the activity of ScRNaseA in function of time is reported after preincubation with PDI (—); PfPDO (—); AaPDO (·····); ApPDO (— · —); control (— — —). The activity of RNaseA against RNA is measured.



tem. These results, the absence of genes encoding glutathione synthesis enzymes from the genomes of other archaea, such as *P. horikoshii*, *P. furiosus*, *A. pernix*, and *S. tokodaii*, and the fact that no GSH or GSSG is found in *P. horikoshii* cell extracts combine to suggest that PDO activity is typical of a non-GSH-dependent system. A chaperone activity has been detected for SsPDO. Compared with the eukaryotic PDI used as a positive control (100), SsPDO was found to catalyze 80% refolding in chemically denatured lysozyme and to perform the same ATPase activity already demonstrated for its homologue, PpPDO (74). In particular, the ATP-dependent refolding activity showed on an endogenous protein, SsADH (*S. solfataricus* alcohol dehydrogenase) (14), suggests a potential role of SsPDO *in vivo*. In addition, the high level of cytosolic disulfide bonds in thermophilic *S. solfataricus* proteins is clear evidence of the extent to which the presence of SsPDO is relevant. All these data taken together indicate that disulfide bond formation and their maintenance is a strategy adopted by *S. solfataricus* to stabilize its proteins and led us to assume that the overall function of SsPDO is to preserve the folded state in cytoplasmic proteins.

Many reports have highlighted the key role of sulfhydryl groups (-SH) in oxidative stress response and, specifically, the role of the Grx/Trx system in the maintenance of cell redox homeostasis (42). To shed further light on the *in vivo* role of SsPDO, the expression of SsPDO was analyzed in oxidative stress. Compared with the marked response to H<sub>2</sub>O<sub>2</sub> observed for the Trx from *Rhodobacter sphaeroides* (55) or the Grx from *E. coli* (78), all the oxidative agents used for the tests produced very small increases in mRNA and protein levels, suggesting that SsPDO is not directly involved in the oxidative stress response.

### Conclusions on the PDO family

Based on its apparent cellular function and the presence of two structural units with an active site each, a link can be drawn between the PDO family and the eukaryotic enzyme, PDI (23, 105). PDI resides in the ER, where it catalyzes the isomerization of protein disulfide bonds in an oxidizing environment. It is possible to speculate that the enzyme used by eukaryotes to form protein disulfide bonds in the ER might have originated from a similar enzyme contained in a disulfide-rich thermophile. Based on these considerations, the members of the PDO family can be considered as the simplest PDI forms found in thermophiles. To test this hypothesis, the theoretic values of the catalytic cysteine pK<sub>a</sub>s of the a and a' domains of yeast PDI have also been calculated (102). The pK<sub>a</sub> values obtained for the N-terminal cysteines of both active sites were found to be lower than those determined for the C-terminal cysteines. Moreover, as already observed for the members of the PDO family, the pK<sub>a</sub> value of the N-terminal cysteine of the a domain was found to be slightly different from that of the a' domain. This difference is in agreement with experimental data, which indicate a higher redox potential for the a' domain (-152 mV) than for the a domain (-188 mV) (102). These findings are further evidence of the functional similarity between the two enzyme families. However, the different three-dimensional organization of the N- and C-terminal units of the PDO family compared with the a and a' domains of PDI strongly point to different

mechanisms of action for these two biologic systems. Hence the need for further experimental studies to clarify how different three-dimensional structures can give rise to similar functional behavior.

## TR/PDO SYSTEM AND ITS INVOLVEMENT IN THE REDOX HOMEOSTASIS

The maintenance of the proper intracellular redox environment in microorganisms is guaranteed by redox and antioxidant systems. TR, a homodimeric flavoenzyme, catalyzes the transfer of reducing equivalents from NADPH to a redox-active disulfide of Trx *via* FAD. On the basis of the differences in size, structure, and catalytic mechanisms, two classes of TR can be distinguished (4). The low-molecular-mass proteins from *E. coli* (106) and *Saccharomyces cerevisiae* (15) are dimers of 35-kDa subunits, whereas the high-molecular-mass proteins from higher eukaryotes, including mammals (29, 101), *C. elegans* (12), and *Plasmodium falciparum* (104) are dimers of 55- to 58-kDa subunits. TRs of both classes are members of a larger family of pyridine nucleotide disulfide oxidoreductases that includes lipoamide dehydrogenase, glutathione reductase, and mercuric reductase (28). The bacterial enzyme is highly specific for the homologous Trx as a substrate (63). In contrast, mammalian TR has a broader substrate specificity and can reduce not only thioredoxins from different species but also many nondisulfides, such as 5,5'-dithiobis(2-nitrobenzoic acid) (DTNB), selenite, selenogluthathione, vitamin K, and alloxan (10, 41). Recently a TR from the hyperthermophilic archaeon *A. pernix* was isolated and characterized (APE1061) (*ApTR*). *ApTR* is phylogenetically closer to the bacterial TRs, showing a relatively high homology to the TR of *E. coli* (34% identity and 54% similarity). *ApTR* possesses two conserved motifs responsible for binding of FAD near the N-terminus (GXGXX [G/A]) and the C-terminus (GXFAAGD) and a NADPH domain near the middle of the protein (GGGXXA), in addition to a redox-active center (CSVC). DTNB, not directly reduced by low-molecular-mass TR (80), can be reduced directly by *ApTR*, indicating that it has a broader substrate specificity than that of low-molecular-mass TRs. *ApTR*/*ApTrx* has been the first example of a functional Trx system in aerobic hyperthermophilic archaea (43). A TR-homologue gene (PH1426) (*PhTR*) was also found in the genome sequence of *P. horikoshii*. The gene was cloned, and the corresponding expressed protein was characterized (47). The protein had some reductase activity against Trx from *E. coli* as well as the redox protein *PhPDO*. *PhTR* is a typical, homodimeric flavoprotein. *PhTR* belongs to the low-molecular-mass class of thioredoxin reductase, because it has a subunit molecular mass of 36 kDa. The apparent K<sub>M</sub> value of *ApTR* for *ApTrx* was  $12.3 \pm 2.7 \mu\text{M}$ , whereas that of *PhTR* for *PhPDO* was  $0.6 \pm 0.02 \mu\text{M}$ , indicating that the affinity of *PhTR* for *PhPDO* is higher than that of *ApTR* for *ApTrx* (43, 47). In an obligate anaerobic archaeon, the high affinity of *PhTR* for *PhPDO* may be essential to maintain a sufficiently low redox potential in the cytoplasm. The *P. horikoshii* Trx system described may also play a critical role in resistance to oxidative stress against traces of oxygen and for the maintenance

of redox homeostasis in the cytoplasm. This is the first report of Grx-homologue protein that directly mediates the electron transfer from a TR-like flavoprotein to protein disulfide in archaea. In some obligate anaerobic bacteria, systems for oxidative-stress response related to some redox-proteins have been found (66, 87, 98).

To better characterize the role of SsPDO, the PDO already cited, recently the Trx system of *S. solfataricus* was investigated in greater detail; investigations of the genomic sequence databases led to the identification of two TRs (*i.e.*, SsTR and Sso2765) (3, 93).

The data reported suggest that SsPDO is part of a Trx-like system that plays a central role in the biochemistry of cytoplasmic disulfide bonds in *S. solfataricus*. The recombinant SsTR, homologous to ApTR, was expressed in *E. coli*. Specific inhibitors of human (33) and mitochondrial (89) TR act on SsTR activities. Conversely, a typical inhibitor of eubacterial TR (33) was almost unable to affect the activity of SsTR. These findings, together with the broad substrate SsTR specificity, active both on DTNB and SsPDO, support the hypothesis that this archaeal enzyme, more structurally related to eubacterial ones, is functionally closer to eukaryal enzymes (109). SsTR was found to be active with SsPDO with a very low value of  $K_M$  (0.3  $\mu M$ , 60°C) with catalytic properties similar to those of the system (PhTR/PhPDO,  $K_M$  0.6  $\mu M$ , 25°C) identified in the anaerobic archaeon *P. horikoshii*. No homology was found for ApTrx in the *S. solfataricus* genome. The  $K_M$  value for ApTR versus Ap-Trx was found to be 12.3  $\mu M$  at 25°C.

The Trx system has been shown to mediate the NAD(P)H-dependent recycling of a ubiquitous family of antioxidant enzymes: the Prxs (Fig. 5). Prxs are divided into three classes: typical 2-Cys Prx, atypical 2-Cys Prx, and 1-Cys Prx (107). All Prxs share the same basic catalytic mechanism, in which an active-site cysteine (the peroxidative cysteine,  $S_P$ ) is oxidized to a sulfenic acid by the peroxide substrate. The recycling of the sulfenic acid back to a thiol is what distinguishes the three enzyme classes.

Prxs exert their protective antioxidant role in cells through their peroxidase activity ( $ROOH$  and  $2e^- \rightarrow ROH + H_2O$ ), whereby hydrogen peroxide, peroxyxynitrite, and a wide range of organic hydroperoxides ( $ROOH$ ) are reduced and detoxified. The redundancy of Prxs in a wide range of cells and a recent finding that a bacterial Prx (AhpC) instead of catalase is responsible for the reduction of endogenously generated  $H_2O_2$  argue that Prxs are important players in peroxide detoxification in cells. The gene, which has some homology to Prx, has been found in archaea such as *Thermoplasma volcanium*, *Thermotoga maritima*, *Thermoplasma acidophilum*, *S. tokodaii*, and *A.*

*pernix*. A gene (APE2278) encoding the Prx homologous protein of yeast and human was identified in the genome of *A. pernix*. The recombinant protein shows peroxidase activity *in vitro* (ApPrx). ApPrx forms a hexadecamer composed of two identical octamers, and its action mechanism appears to be identical to that of 2-Cys Prx (44, 65). The novel oligomeric structure may represent a tactic for getting a multifunctional antioxidant system and achieving hyperthermostability. ApPrx, reflecting ancestral features of an antioxidant defense system, is dependent on a NADPH/ApTR/ApTrx system to reduce  $H_2O_2$  *in vitro*.

Another archaeal Prx from *P. horikoshii* (PH1217) (46, 48) was recently characterized and subsumed within the 2-Cys family. PH1217 has peroxidase activity, but the electron donor partner might be different from that found in *A. pernix* because in the genome database of *P. horikoshii* were not found either a homologue of *A. pernix* Trx-like or other types of Trxs.

The genome analysis of the archaeon *S. solfataricus* showed the absence of putative catalases and the presence of four putative Prxs: Bcp1, Bcp2, Bcp3, and Bcp4, the roles of which should be clarified in detail and which could play a key function in the detoxification processes. Sequence analysis suggested the classification of Bcp2 and Bcp3 in 1-Cys Prx, but Bcp1 and Bcp4 in 2-Cys Prx. The involvement of the Bcp2 as scavenger of peroxide has been demonstrated, but the physiologic partner in the recycling of this enzyme has not been found (56). The presence of 2-Cys Prxs and the novel SsPDO/SsTR system, recently characterized in *S. solfataricus*, suggest that this redox system could be the physiologic partner in the detoxification of the peroxide, although studies in this direction are necessary to demonstrate it.

## CONCLUSIONS

Important progress has been made over the past several years toward understanding how disulfide bonds are formed in cellular proteins in the ER of eukaryotes and the periplasmic space of prokaryotes. Striking similarities have been revealed between the eukaryotic and prokaryotic protein oxidation and reduction pathways at functional, mechanistic, and structural levels. In this field, the discovery of a new family of protein disulfide oxidoreductases suggested a new and important role of the disulfide bonds in thermophilic proteins as structural stabilizing agents of intracellular proteins. Numerous problems related to protein disulfide oxidoreductases in thermophiles remain unsolved but can probably successfully be studied by genetic and

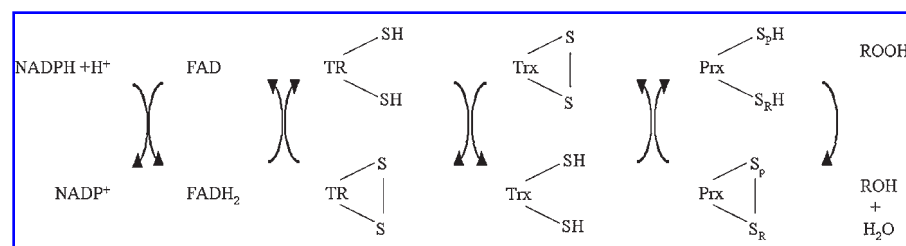


**FIG. 5. Mechanism of peroxide reduction by 2cys-Prx and NADPH/TR/Trx redox system.** In the presence of peroxide, the peroxidative cysteine ( $S_P$ ) of Prx condenses to form a disulfide bond with the second cysteine (resolving cysteine,  $S_R$ ). Reduction of 2-Cys Prxs involves protein or domain containing a CXXC motif, such as Trx, TR, and NADPH.

*in vivo* approaches. How would the phenotype of a thermophilic microorganism react on a knockout of a PDO gene? What are the pathways and the regulation mechanisms for PDO-dependent protein disulfide formation in thermophilic microorganisms? What is the global redox potential in these cells? The study in the model systems, as well as *S. solfataricus* and *P. horikoshii*, has allowed us to answer to some of these questions, among them the reduction system for PDOs, but the physiologic substrates and the peptide-binding regions remain to be elucidated. Overall, understanding the molecular mechanism of PDO function will help to complete a considerable part of the complex puzzle of oxidative protein folding in the cell. In turn, a better understanding of *in vivo* protein folding could have an impact on protein engineering in basic research, industry, and medicine, and could help to unravel the molecular basis of diseases arising from protein misfolding.

## ACKNOWLEDGMENTS

This work was supported by grants from MIUR (PRIN 2003-2004).

## ABBREVIATIONS

Dsb, disulfide bond forming; DTT, dithiothreitol; ER, endoplasmic reticulum; Grx, glutaredoxin; GSH, reduced glutathione; GSSG, GSH oxidized form; PDI, protein disulfide isomerase; PDO, protein disulfide oxidoreductase; Prx, peroxidoreductase; TR, thioredoxin reductase; Trx, thioredoxin.

## REFERENCES

- Amegbey GY, Monzavi H, Habibi-Nazhad B, Bhattacharyya S, and Wishart DS. Structural and functional characterization of a thioredoxin-like protein (Mt0807) from *Methanobacterium thermoautotrophicum*. *Biochemistry* 42: 8001–8010, 2003.
- Anken E and Braakman I. Versatility of the endoplasmic reticulum protein folding factory. *Crit Rev Biochem Mol Biol* 40, 191–228, 2005.
- Arcari P, Fasullo L, Masullo M, Catanzano F, and Bocchini V. A NAD(P)H oxidase isolated from the archaeon *Sulfolobus solfataricus* is not homologous with another NADH oxidase present in the same microorganism biochemical characterization of the enzyme and cloning of the encoding gene. *J Biol Chem* 275: 895–900, 2000.
- Arscott LD, Gromer S, Schirmer RH, Becker K, and Williams CH Jr. The mechanism of thioredoxin reductase from human placenta is similar to the mechanisms of lipoamide dehydrogenase and glutathione reductase and is distinct from the mechanism of thioredoxin reductase from *Escherichia coli*. *Proc Natl Acad Sci U S A* 94: 3621–3626, 1997.
- Bartolucci S, Guagliardi A, Pedone E, De Pascale D, Cannio R, Camardella L, Rossi M, Nicastro G, de Chiara C, Facci P, Mascetti G, and Nicolini C. Thioredoxin from *Bacillus acidocaldarius*: characterization, high-level expression in *Escherichia coli* and molecular modelling. *Biochem J* 328: 277–285, 1997.
- Bartolucci S, De Pascale D, and Rossi M. Protein disulfide oxidoreductase from *Pyrococcus furiosus*: biochemical properties. *Methods Enzymol* 334: 62–73, 2001.
- Bartolucci S, De Simone G, Galdiero S, Improta R, Menchise V, Pedone C, Pedone E, and Saviano M. An integrated structural and computational study of the thermostability of two thioredoxin mutants from *Alicyclobacillus acidocaldarius* *J Bacteriol* 185: 4285–4289, 2003.
- Beeby M, O'Connor BD, Ryttersgaard C, Boutz DR, Perry LJ, and Yeates TO. The genomics of disulfide bonding and protein stabilization in thermophiles. *PLoS Biol* 3: 1549–1558, 2005.
- Bhattacharyya S, Habibi-Nazhad B, Amegbey G, Slupsky CM, Yee A, Arrowsmith C, and Wishart DS. Identification of a novel archaeobacterial thioredoxin: determination of function through structure. *Biochemistry* 41: 4760–4770, 2002.
- Bjornstedt M, Hamberg M, Kumar S, Xue, J, and Holmgren A. Human thioredoxin reductase directly reduces lipid hydroperoxides by NADPH and selenocystine strongly stimulates the reaction via catalytically generated selenols. *J Biol Chem* 270: 11761–11764, 1995.
- Bjornstedt M, Kumar S, Bjorkhem L, Spyrou G, and Holmgren A. Selenium and the thioredoxin and glutaredoxin systems. *Bio-med Environ Sci* 10: 271–279, 1997.
- Buettner C, Harney JW, and Berry M.J. The *Caenorhabditis elegans* homologue of thioredoxin reductase contains a selenocysteine insertion sequence (SECIS) element that differs from mammalian SECIS elements but directs selenocysteine incorporation. *J Biol Chem* 274: 21598–21602, 1999.
- Cabibbo A, Pagani M, Fabbri M, Rocchi M, Farmery MR, Bulleid NJ, and Sitia R. ERO1-L, a human protein that favors disulfide bond formation in the endoplasmic reticulum. *J Biol Chem* 275: 4827–4833, 2000.
- Cannio R, Fiorentino G, Carpinelli P, Rossi M, and Bartolucci S. Cloning and overexpression in *Escherichia coli* of the genes encoding NAD-dependent alcohol dehydrogenase from two *Sulfolobus* species. *J Bacteriol* 178: 301–305, 1996.
- Chae HZ, Chung SJ, and Rhee SG. Thioredoxin dependent peroxide reductase from yeast. *J Biol Chem* 269: 27670–27678, 1994.
- D'Ambrosio K, De Simone G, Pedone E, Rossi M, Bartolucci S, and Pedone C. Crystallization and preliminary X-ray diffraction studies of a protein disulfide oxidoreductase from *Aquifex aeolicus*. *Acta Cryst D60*: 2076–2077, 2004.
- D'Ambrosio K, De Simone G, Pedone E, Rossi M, Bartolucci S, and Pedone C. Crystallization and preliminary X-ray diffraction studies of a protein disulfide oxidoreductase from *Aeropyrum pernix* K1. *Acta Cryst F61*: 335–336, 2005.
- D'Ambrosio K, Pedone E, Langella E, De Simone G, Rossi M, Pedone C, and Bartolucci S. A novel member of the protein disulfide oxidoreductase family from *Aeropyrum pernix* K1: structure, function and electrostatics. *J Mol Biol* 362: 743–752, 2006.
- Darby NJ, Kemmink J, and Creighton TE. Identifying and characterizing a structural domain of protein disulfide isomerase. *Biochemistry* 35: 10517–10522, 1996.
- Dijkstra K, Karvonen P, Pirneskoski A, Koivunen P, Kivirikko KI, Darby NJ, van Straaten M, Scheek RM, and Kemmink J. Assignment of 1H, 13C and 15N resonances of the a' domain of protein disulfide isomerase. *J Biomol NMR* 14: 195–196, 1999.
- Dixon DP, Van Lith M, Edwards R, and Benham A. Cloning and initial characterization of the *Arabidopsis thaliana* endoplasmic reticulum oxidoreductins. *Antioxid Redox Signal* 5: 389–396, 2003.
- Fabianek RA, Hennecke H, and Thony-Meyer L. Periplasmic protein thiol:disulfide oxidoreductases of *Escherichia coli*. *FEMS Microbiol Rev* 24: 303–316, 2000.
- Ferrari DM and Soling HD. The protein disulphide-isomerase family: unraveling a string of folds. *Biochem J* 339: 1–10, 1999.
- Freedman RB. Novel disulfide oxidoreductase in search of a function. *Nat Struct Biol* 5: 531–532, 1998.
- Freedman RB, Klappa P, and Ruddock LW. Protein disulfide isomerases exploit synergy between catalytic and specific binding domains. *EMBO Rep* 3: 136–140, 2002.
- Fuchs JA. Glutathione: chemical, biochemical, and medical aspects. Edited by Dolphin D, Poulsen R, and Avramovic O. New York: John Wiley and Sons, 1989 Part B, p 551.
- Ghaemmaghami S, Huh WK, Bower K, Howson RW, Belle A, Dephoure N, O'Shea EK, and Weissman JS. Global analysis of protein expression in yeast. *Nature* 425: 737–741, 2003.



28. Ghisla S and Massey V. Mechanisms of flavoprotein catalyzed reactions. *Eur J Biochem* 181: 1–17, 1989.
29. Gladyshev VN, Jeang KT, and Stadtman TC. Selenocysteine, identified as the penultimate C-terminal residue in human T-cell thioredoxin reductase, corresponds to TGA in the human placental gene. *Proc Natl Acad Sci U S A* 93: 6146–6151, 1996.
30. Gleason FK and Holmgren A. Thioredoxin and related proteins in procaryotes. *FEMS Microbiol Rev* 4: 271–297, 1988.
31. Grauschopf U, Winther JR, Korber P, Zander T, Dallinger P, and Bardwell JC. Why is DsbA such an oxidizing disulfide catalyst? *Cell* 83: 947–955, 1995.
32. Grauschopf U, Fritz A, and Glockshuber R. Mechanism of the electron transfer catalyst DsbB from *Escherichia coli*. *EMBO J* 22: 3503–3513, 2003.
33. Gromer S, Merkle H, Schirmer RH, and Becker K. Human placenta thioredoxin reductase: preparation and inhibitor studies. *Methods Enzymol* 347: 382–394, 2002.
34. Gross E, Sevier CS, Vala A, Kaiser CA, and Fass D. A new FAD-binding fold and intersubunit disulfide shuttle in the thiol oxidase Erv2p. *Nat Struct Biol* 9: 61–67, 2002.
35. Gross E, Kastner DB, Kaiser CA, and Fass D. Structure of Ero1p, source of disulfide bonds for oxidative protein folding in the cell. *Cell* 117: 601–610, 2004.
36. Gross E, Sevier CS, Heldman N, Vitu E, Bentzur M, Kaiser CA, Thorpe C, and Fass D. Generating disulfides enzymatically: reaction products and electron acceptors of the endoplasmic reticulum thiol oxidase Ero1p. *Proc Natl Acad Sci U S A* 103: 299–304, 2006.
37. Guagliardi A, De Pascale D, Cannio R, Nobile V, Bartolucci S, and Rossi M. The purification, cloning, and high level expression of a glutaredoxin-like protein from the hyperthermophilic archaeon *Pyrococcus furiosus*. *J Biol Chem* 270: 5748–5755, 1995.
38. Guthapfel R, Gueguen P, and Quemeneur E. ATP binding and hydrolysis by the multifunctional protein disulfide isomerase. *J Biol Chem* 271:2663–2666, 1996.
39. Holmgren A. Thioredoxin. *Annu Rev Biochem* 54: 237–271, 1985.
40. Holmgren A. Thioredoxin and glutaredoxin: small multi-functional redox proteins with active-site disulphide bonds. *Biochem Soc Trans* 16: 95–96, 1988.
41. Holmgren A and Bjornstedt M. Thioredoxin and thioredoxin reductase. *Methods Enzymol* 252: 199–208, 1995.
42. Holmgren A, Johansson C, Berndt C, Lonn ME, Hudemann C, and Lillig CH. Thiol redox control via thioredoxin and glutaredoxin systems. *Biochem Soc Trans* 33: 1375–1377, 2005.
43. Jeon SJ and Ishikawa K. Identification and characterization of thioredoxin and thioredoxin reductase from *Aeropyrum pernix* K1. *Eur J Biochem* 269: 5423–5430, 2002.
44. Jeon SJ and Ishikawa K. Characterization of novel hexadecameric thioredoxin peroxidase from *Aeropyrum pernix* K1. *J Biol Chem* 278: 24174–24180, 2003.
45. Kadokura H, Katzen F, and Beckwith J. Protein disulfide bond formation in prokaryotes. *Annu Rev Biochem* 72: 111–135, 2003.
46. Kashima Y and Ishikawa K. Alkyl hydroperoxide reductase dependent on thioredoxin-like protein from *Pyrococcus horikoshii*. *J Biochem (Tokyo)* 134: 25–29, 2003.
47. Kashima Y and Ishikawa K. A hyperthermostable novel protein-disulfide oxidoreductase is reduced by thioredoxin reductase from hyperthermophilic archaeon *Pyrococcus horikoshii*. *Arch Biochem Biophys* 418: 179–185, 2003.
48. Kawakami R, Sakuraba H, Kamohara S, Goda S, Kawarabayashi Y, and Ohshima T. Oxidative stress response in an anaerobic hyperthermophilic archaeon: presence of a functional peroxiredoxin in *Pyrococcus horikoshii*. *J Biochem (Tokyo)* 136: 541–547, 2004.
49. Kemmink J, Darby NJ, Dijkstra K, Nilges M, and Creighton TE. Structure determination of the N-terminal thioredoxin-like domain of protein disulfide isomerase using multidimensional heteronuclear <sup>13</sup>C/<sup>15</sup>N NMR spectroscopy. *Biochemistry* 35: 7684–7691, 1996.
50. Kemmink J, Dijkstra K, Mariani M, Scheek RM, Penka E, Nilges M, and Darby NJ. The structure in solution of the b domain of protein disulfide isomerase. *J Biomol NMR* 13: 357–368, 1999.
51. Kortemme T, Darby NJ, and Creighton TE. Electrostatic interactions in the active site of the N-terminal thioredoxin-like domain of protein disulfide isomerase. *Biochemistry* 35: 14503–14511, 1996.
52. Lappi A, Lensink M, Alanen H, Salo K, Lobell M, Juffer A, and Ruddock L. A conserved arginine plays a role in the catalytic cycle of the protein disulphide isomerases. *J Mol Biol* 335: 283–295, 2004.
53. Lee DY, Ahn BY, and Kim KS. A thioredoxin from the hyperthermophilic archaeon *Methanococcus jannaschii* has a glutaredoxin-like fold but thioredoxin-like activities. *Biochemistry* 39: 6652–6659, 2000.
54. Lemaire SD and Miginiac-Maslow M. The thioredoxin superfamily in *Chlamydomonas reinhardtii*. *Photosynth Res* 82: 203–220, 2004.
55. Li K, Pasternak C, and Klug G. Expression of the *trx*A gene for thioredoxin 1 in *Rhodobacter sphaeroides* during oxidative stress. *Arch Microbiol* 180: 484–489, 2003.
56. Limauro D, Pedone E, Pirone L, and Bartolucci S. Identification and characterization of 1-Cys peroxiredoxin from *Sulfolobus solfataricus* and its involvement in the response to oxidative stress. *FEBS J* 273: 721–731, 2006.
57. Mallick P, Boutz DR, Eisenberg D, and Yeates T O. Genomic evidence that the intracellular proteins of archaeal microbes contain disulfide bonds. *Proc Natl Acad Sci U S A* 99: 9679–9684, 2002.
58. Martin JL, Bardwell JC, and Kuriyan J. Crystal structure of the DsbA protein required for disulphide bond formation in vivo. *Nature* 365: 464–468, 1993.
59. Martin JL. Thioredoxin: a fold for all reasons. *Structure* 3: 245–250, 1995.
60. McFarlan SC, Terrell CA, and Hogenkamp HP. The purification, characterization, and primary structure of a small redox protein from *Methanobacterium thermoautotrophicum*, an archaeobacterium. *J Biol Chem* 267: 10561–10569, 1992.
61. Meister A. Glutathione metabolism and its selective modification. *J Biol Chem* 263: 17205–17208, 1988.
62. Messens J and Collet JF. Pathways of disulfide bond formation in *Escherichia coli*. *Int J Biochem Cell Biol* 38: 1050–1062, 2006.
63. Miranda-Vizuet A, Damdimopoulos AE, Gustafsson J, and Spyrou G. Cloning, expression, and characterization of a novel *Escherichia coli* thioredoxin. *J Biol Chem* 272: 30841–30847, 1997.
64. Mittard V, Blackledge MJ, Stein M, Jacquot JP, Marion D, and Lancelin JM. NMR solution structure of an oxidised thioredoxin h from the eukaryotic green alga *Chlamydomonas reinhardtii*. *Eur J Biochem* 243: 374–383, 1997.
65. Mizohata E, Sakai H, Fusatomi E, Terada T, Murayama K, Shirouzu M, and Yokoyama S. Crystal structure of an archaeal peroxiredoxin from the aerobic hyperthermophilic crenarchaeon *Aeropyrum pernix* K1. *J Mol Biol* 354: 317–329, 2005.
66. Moore EC, Reichard P, and Thelander L. Enzymatic synthesis of deoxyribonucleotides.V. Purification and properties of thioredoxin reductase from *Escherichia coli* B. *J Biol Chem* 239: 3445–3452, 1964.
67. Moutevelis E and Warwickwe J. Prediction of pKa and redox properties in the thioredoxin superfamily. *Protein Sci* 13: 2744–2752, 2004.
68. Nicastro G, de Chiara C, Pedone E, Tato' M, Rossi M, and Bartolucci S. NMR solution structure of a novel thioredoxin from *Bacillus acidocaldarius*: possible determinants of protein stability. *Eur J Biochem* 267: 403–413, 2000.
69. Pagani M, Fabbri M, Benedetti C, Fassio A, Pilati S, Bulleid NJ, Cabibbo A, and Sitia R. Endoplasmic reticulum oxidoreductin 1-lb (ERO1-Lb), a human gene induced in the course of the unfolded protein response. *J Biol Chem* 275: 23685–23692, 2000.
70. Pedone E, Bartolucci S, Rossi M, and Saviano M. Computational analysis of the thermal stability in thioredoxins: a molecular dynamics approach. *J Biomol Struct Dynamics* 16: 437–446, 1998.
71. Pedone E, Cannio R, Saviano M, Rossi M, and Bartolucci S. Prediction and experimental testing of *Bacillus acidocaldarius* thioredoxin stability. *Biochem J* 339: 309–317, 1999.
72. Pedone E, Saviano M, Rossi M, and Bartolucci S. A single point mutation Glu85Arg enhances the thermostability of the thioredoxin from *Escherichia coli*. *Protein Eng* 14: 255–260, 2001.
73. Pedone E, Bartolucci S, Rossi M, Pierfederici FM, Scirè A, Cacciamani T, and Tanfani F. Structural and thermal stability analysis of *Escherichia coli* and *Alicyclobacillus acidocaldarius* thioredoxin revealed a molten globule-like state in thermal denaturation pathway of the proteins: an infrared spectroscopic study. *Biochem J* 373: 875–883, 2003.



74. Pedone E, Ren B, Ladenstein R, Rossi M, and Bartolucci S. Functional properties of the protein disulfide oxidoreductase from the archaeon *Pyrococcus furiosus*. *Eur J Biochem* 271: 3437–3448, 2004.
75. Pedone E, Saviano M, Bartolucci S, Rossi M, Ausili A, Scire A, Bertoli E, and Tanfani F. Temperature, SDS-, and pH-induced conformational changes in protein disulfide oxidoreductase from the archaeon *Pyrococcus furiosus*: a dynamic simulation and Fourier transform infrared spectroscopic study. *J Proteome Res* 4: 1972–1980, 2005.
76. Pedone E, D'Ambrosio K, De Simone G, Rossi M, Pedone C, and Bartolucci S. Insights on a new PDI-like family: structural and functional analysis of a protein disulfide oxidoreductase from the bacterium *Aquifex aeolicus*. *J Mol Biol* 356: 155–164, 2006.
77. Pedone E, Limauro D, D'Alterio R, Rossi M, and Bartolucci S. Characterization of a multifunctional protein disulfide oxidoreductase from *Sulfolobus solfataricus*. *FEBS J* 273: 5407–5420, 2006.
78. Prieto-Alamo MJ, Jurado J, Gallardo-Madueno R, Monje-Casas F, Holmgren A, and Pueyo C. Transcriptional regulation of glutaredoxin and thioredoxin pathways and related enzymes in response to oxidative stress. *J Biol Chem* 275: 13398–13405, 2000.
79. Prinz WA, Aslund F, Holmgren A, and Beckwith J. The role of the thioredoxin and glutaredoxin pathways in reducing protein disulfide bonds in the *Escherichia coli* cytoplasm. *J Biol Chem* 272: 15661–15667, 1997.
80. Prongay AJ, Engelke DR, and Williams CH Jr. Characterization of two active site mutations of thioredoxin reductase from *Escherichia coli*. *J Biol Chem* 264: 2656–2664, 1989.
81. Quemener E, Guthapfel R, and Gueguen P. A major phosphoprotein of the endoplasmic reticulum is protein disulfide isomerase. *J Biol Chem* 269: 5485–5488, 1994.
82. Raczko AM, Bujnicki JM, Pawlowski M, Godlewska R, Lewandowska M, and Jagusztyn-Krynicka EK. Characterization of new DsbB-like thiol-oxidoreductases of *Campylobacter jejuni* and *Helicobacter pylori* and classification of the DsbB family based on phylogenomic, structural and functional criteria. *Microbiology* 151: 219–223, 2005.
83. Rehse PH, Kumei M, and Tahirov TH. Compact reduced thioredoxin structure from the thermophilic bacteria *Thermus thermophilus*. *Proteins* 61:1032–1037, 2005.
84. Ren B, Tibbelin G, De Pascale D, Rossi M, Bartolucci S, and Ladenstein R. Crystallization and preliminary X-ray structure analysis of a hyperthermostable thioltransferase from the archaeon *Pyrococcus furiosus*. *J Struct Biol* 119: 1–5, 1997.
85. Ren B, Tibbelin G, De Pascale D, Rossi M, Bartolucci S, and Ladenstein R. A protein disulfide oxidoreductase from the archaeon *Pyrococcus furiosus* contains two thioredoxin fold units. *Nat Struct Biol* 5: 602–611, 1998.
86. Ren B and Ladenstein R. Protein disulfide oxidoreductase from *Pyrococcus furiosus*: structural properties. *Methods Enzymol* 334: 74–88, 2001.
87. Reynolds CM, Meyer J, and Poole LB. An NADH-dependent bacterial thioredoxin reductase-like protein in conjunction with a glutaredoxin homologue form a unique peroxiredoxin (AhpC) reducing system in *Clostridium pasteurianum*. *Biochemistry* 41: 1990–2001, 2002.
88. Rietsch A, Belin D, Martin N, and Beckwith J. An in vivo pathway for disulfide bond isomerization in *Escherichia coli*. *Proc Natl Acad Sci U S A* 93: 13048–13053, 1996.
89. Rigobello MP, Scutari G, Folda A and Bindoli A. Mitochondrial thioredoxin reductase inhibition by gold(I) compounds and concurrent stimulation of permeability transition and release of cytochrome c. *Biochem Pharmacol* 67: 689–696, 2004.
90. Rossmann R, Stern D, Lofrer H, Jacobi A, Glockshuber R, and Hennecke H. Replacement of Pro109 by His in TlpA, a thioredoxin-like protein from *Bradyrhizobium japonicum*, alters its redox properties but not its in vivo functions. *FEBS Lett* 406: 249–254, 1997.
91. Rouhier N, Gelhaye E, Sautiere PE, Brun A, Laurent P, Tagu D, Gerard J, de Fay E, Meyer Y, and Jacquot JP. Isolation and characterization of a new peroxiredoxin from poplar sieve tubes that uses either glutaredoxin or thioredoxin as a proton donor. *Plant Physiol* 127:1299–1309, 2001.
92. Ruddock LW, Hirst TR, and Feedman RB. pH-dependence of the dithiol-oxidizing activity of DsbA (a periplasmic protein thiol:disulphide oxidoreductase) and protein disulphide-isomerase: studies with a novel simple peptide substrate. *Biochem J* 315: 1000–1005, 1995.
93. Ruocco MR, Ruggiero A, Masullo L, Arcari P, and Masullo M. A 35 kDa NAD(P)H oxidase previously isolated from the archaeon *Sulfolobus solfataricus* is instead a thioredoxin reductase. *Biochimie* 86: 883–892, 2004.
94. Saarinen M, Gleason FK, and Eklund H. Crystal structure of thioredoxin-2 from *Anabaena*. *Structure* 3: 1097–1108, 1995.
95. Sevier CS, Cuozzo JW, Vala A, Aslund F, and Kaiser CA. A flavoprotein oxidase defines a new endoplasmic reticulum pathway for biosynthetic disulphide bond formation. *Nat Cell Biol* 3: 874–882, 2001.
96. Sevier CS and Kaiser CA. Disulfide transfer between two conserved cysteine pairs imparts selectivity to protein oxidation by Ero1. *Mol Biol Cell* 17: 2256–2266, 2006.
97. She Q, Singh RK, Confalonieri F, Zivanovic Y, Allard G, Awayez M J, Chan-Weiher CC, Clausen IG, Curtis BA, De Moors A., Eraso G, Fletcher C, Gordon PM, Heikamp-de Jong I, Jeffries AC, Kozera CJ, Medina N, Peng X, Thi-Ngoc HP, Redder P, Schenk ME, Theriault C, Tolstrup N, Charlebois RL, Doolittle WF, Duguet M, Gaasterland T, Garrett RA, Ragan MA, Sensen CW, and Van der Oost J. The complete genome of the crenarchaeon *Sulfolobus solfataricus* P2. *Proc Natl Acad Sci U S A* 8: 7835–7840, 2001.
98. Silva G, LeGall J, Xavier AV, Teixeira M, and Rodrigues-Poussada C. Molecular characterization of *Desulfovibrio gigas* neolaredoxin, a protein involved in oxygen detoxification in anaerobes. *J Bacteriol* 183: 4413–4420, 2001.
99. Sitia R and Braakman I. Quality control in the endoplasmic reticulum protein factory. *Nature* 426: 891–894, 2003.
100. Song J, Quan H, and Wang C. Dependence of anti-chaperone activity of protein disulphide isomerase on its chaperone activity. *Biochem J* 328: 841–846, 1997.
101. Tamura T and Stadtman TC. A new selenoprotein from human lung adenocarcinoma cells: purification, properties, and thioredoxin reductase activity. *Proc Natl Acad Sci U S A* 3:1006–1011, 1996.
102. Tian G, Xiang S, Noiva R, Lennarz WJ, and Schindelin H. The crystal structure of yeast protein disulfide isomerase suggests cooperativity between its active sites. *Cell* 124: 61–73, 2006.
103. Vala A, Sevier CS, and Kaiser CA. Structural determinants of substrate access to the disulfide oxidase Erv2p. *J Mol Biol* 354: 952–966, 2005.
104. Wang PF, Arscott LD, Gilberger TW, Muller S, and Williams CH Jr. Thioredoxin reductase from *Plasmodium falciparum*: evidence for interaction between the C-terminal cysteine residues and the active site disulfide-dithiol. *Biochemistry* 38: 3187–3196, 1999.
105. Wilkinson B and Gilbert HF. Protein disulfide isomerase. *Biochim Biophys Acta* 1699: 35–44, 2004.
106. Williams CH Jr. Mechanism and structure of thioredoxin reductase from *Escherichia coli*. *FASEB J* 9: 1267–1276, 1995.
107. Wood ZA, Schroder E, Robin Harris J, and Poole LB. Structure, mechanism and regulation of peroxiredoxins. *Trends Biochem Sci* 28: 32–40, 2003.
108. Wunderlich M and Glockshuber R. Redox properties of protein disulfide isomerase (DsbA) from *Escherichia coli*. *Protein Sci* 2: 717–726, 1993.
109. Zillig W, Palm P, Reiter WD, Gropp F, Puhler G, and Klenk HP. Comparative evaluation of gene expression in archaebacteria. *Eur J Biochem* 173: 473–482, 1988.

Address reprint requests to:

Emilia Pedone

Istituto di Biostrutture e Bioimmagini, C.N.R.

Via Mezzocannone 16

80134 Naples, Italy

E-mail: empedone@unina.it

Date of first submission to ARS Central, July 27, 2007; date of acceptance, July 31, 2007.



**This article has been cited by:**

1. Mirva J. Saaranen , Lloyd W. Ruddock . Disulfide Bond Formation in the Cytoplasm. *Antioxidants & Redox Signaling*, ahead of print. [[Abstract](#)] [[Full Text HTML](#)] [[Full Text PDF](#)] [[Full Text PDF with Links](#)]
2. Yoshimi Sato, Kenji Inaba. 2012. Disulfide bond formation network in the three biological kingdoms, bacteria, fungi and mammals. *FEBS Journal* **279**:13, 2262-2271. [[CrossRef](#)]
3. Lloyd W. Ruddock . 2012. Low-Molecular-Weight Oxidants Involved in Disulfide Bond Formation. *Antioxidants & Redox Signaling* **16**:10, 1129-1138. [[Abstract](#)] [[Full Text HTML](#)] [[Full Text PDF](#)] [[Full Text PDF with Links](#)]
4. Giovanna Cacciapuoti, Anna Marabotti, Francesca Fuccio, Marina Porcelli. 2011. Unraveling the structural and functional differences between purine nucleoside phosphorylase and 5#-deoxy-5#-methylthioadenosine phosphorylase from the archaeon *Pyrococcus furiosus*. *Biochimica et Biophysica Acta (BBA) - Proteins and Proteomics* **1814**:10, 1358-1366. [[CrossRef](#)]
5. Stefano M. Marino , Vadim N. Gladyshev . 2011. Redox Biology: Computational Approaches to the Investigation of Functional Cysteine Residues. *Antioxidants & Redox Signaling* **15**:1, 135-146. [[Abstract](#)] [[Full Text HTML](#)] [[Full Text PDF](#)] [[Full Text PDF with Links](#)]
6. Julien Jorda, Todd O. Yeates. 2011. Widespread Disulfide Bonding in Proteins from Thermophilic Archaea. *Archaea* **2011**, 1-9. [[CrossRef](#)]
7. Emilia Pedone, Danila Limauro, Katia D'Ambrosio, Giuseppina Simone, Simonetta Bartolucci. 2010. Multiple catalytically active thioredoxin folds: a winning strategy for many functions. *Cellular and Molecular Life Sciences* **67**:22, 3797-3814. [[CrossRef](#)]
8. Emilia Pedone , Danila Limauro , Simonetta Bartolucci . 2010. Corrigendum for Pedone E, Limauro D, and Bartolucci S. The Machinery for Oxidative Protein Folding in Thermophiles. *Antioxid Redox Signal* 10:157–169, 2008. *Antioxidants & Redox Signaling* **12**:1, 171-179. [[Citation](#)] [[Full Text HTML](#)] [[Full Text PDF](#)] [[Full Text PDF with Links](#)]
9. Giovanna Cacciapuoti, Iolanda Peluso, Francesca Fuccio, Marina Porcelli. 2009. Purine nucleoside phosphorylases from hyperthermophilic Archaea require a CXC motif for stability and folding. *FEBS Journal* **276**:20, 5799-5805. [[CrossRef](#)]
10. Katia D'Ambrosio, Danila Limauro, Emilia Pedone, Ilaria Galdi, Carlo Pedone, Simonetta Bartolucci, Giuseppina De Simone. 2009. Insights into the catalytic mechanism of the Bcp family: Functional and structural analysis of Bcp1 from *Sulfolobus solfataricus*. *Proteins: Structure, Function, and Bioinformatics* **76**:4, 995-1006. [[CrossRef](#)]
11. Danila Limauro, Emilia Pedone, Ilaria Galdi, Simonetta Bartolucci. 2008. Peroxiredoxins as cellular guardians in *Sulfolobus solfataricus*— characterization of Bcp1, Bcp3 and Bcp4. *FEBS Journal* **275**:9, 2067-2077. [[CrossRef](#)]
12. Salvador Ventura . 2008. Oxidative Protein Folding: From the Test Tube to In Vivo Insights. *Antioxidants & Redox Signaling* **10**:1, 51-54. [[Citation](#)] [[Full Text PDF](#)] [[Full Text PDF with Links](#)]